Research Article | Vol. 29, No. 3 / 1 February 2021 / Optics Express 2953
Optics EXPRESS

Diffraction analysis of multiple-disk occulters in external coronagraphs based on uniform boundary wave diffraction theory

WEI WANG,[1,*] XIN ZHANG,[1] QINGYU MENG,[1,2] AND DONG WANG[1]

[1] *Changchun Institute of Optics, Fine Mechanics and Physics, Chinese Academy of Sciences, No. 3888, Dongnanhu Road, Changchun 130033, China*
[2] *Research Center for Space Optical Engineering, Harbin Institute of Technology, Harbin 150000, China*
[*] *wangwei123@ciomp.ac.cn*

Abstract: Occulters with multiple-disk structure are commonly used for mitigating the diffraction light from specific incident angles in external coronagraphs. In the design phase of coronagraphs, it is of great importance to calculate the diffraction propagation of the occulters with high accuracy and high efficiency. In this paper, an analytical method is proposed for the diffraction analysis of multiple-disk occulters based on uniform boundary wave (BDW) diffraction theory. First, an analytical propagator with Fresnel functions is derived for single-disk case, of which the accuracy and efficiency are demonstrated by a numerical example. Then it is proved that the propagator in multiple-disk case was just the iterative use of the single-disk one when neglecting the gradient diffraction term. The analytical propagator presents much improvement on simplification and efficiency compared to former numerical propagators, and hence, is of great significance to future external coronagraph design and analysis.

1. Introduction

Occulters with multiple-disk structure are commonly used for mitigating the diffraction light from specific incident angles in external coronagraphs. First proposed in [1], multiple-disk external occulters were successfully used in former solar exploration missions, such as the SMM [2], LASCO-C2 [3] and SECCHI-COR2 [4]. The performance of coronagraphs is mainly subject to the constraint brought by the halo of diffraction from the direct sunlight [5]. During the initial design phase, calculating the diffraction propagation with high accuracy and high efficiency will contribute to better evaluation of the performance and shorten the time of iterative designs.

To achieve this goal, various methods have been proposed for the analysis of diffraction effects by external occulters in solar coronagraphs, which can be roughly divided into two types. The first one is based on Fresnel-Kirchoff wavelet integral. In circular symmetric case, the Fresnel-Kirchoff integral can be expressed as a 1-dimensional integral with Bessel functions [6]. Recently, Aime proposed the analytical expression of Fresnel-Kirchoff integral in two-disk diffraction case and gave a numerical demonstration [7]. An analytical propagator for three or more disks diffraction, which is the same goal of this paper, was given but was not numerically demonstrated since the form is much too complex. Another method is based on boundary wave (BDW) diffraction theory. In [8], Lenskii derived the expression of boundary wave integral for the case of multiple-disk external occulters, and provided the solution at the on-axis point instead of a feasible numerical algorithm for general diffraction fields. In [9], Rougeot and Aime proposed a BDW integral representation for serrated external occulters. In stellar coronagraph, BDW theory has been also successfully used for diffraction analysis [10][11]. High order BDW formulation over multiple apertures has been theoretically and experimentally studied in [12] and [13]. However, this formulation cannot be used in the multiple-disk case.

#408524 https://doi.org/10.1364/OE.408524
Journal © 2021 Received 31 Aug 2020; revised 19 Nov 2020; accepted 20 Nov 2020; published 19 Jan 2021

According to BDW theory, the diffraction fields can be described as the sum of two terms, i.e., the boundary diffraction waves along the occulter's boundary in the form of 1D integral, and the geometrically incident wave depending on the situation. In the sense of mathematics, the boundary wave integral is equivalent to the Fresnel-Kirchoff integral with the Stokes transformation [14]. In most cases, using BDW theory to calculate diffraction effects is more efficient, as proved by Rougeot [5], due to the existence of one oscillating term e^{jkS} in the 1D integral. While the nature of Fresnel-Kirchoff integral is 2D, and when being simplified to 1D it will induce another oscillating term Bessel function. Calculation efficiency is more important in multiple-disk diffraction due to the fact that the calculation process will be iteratively used for several times. Nevertheless, an intrinsic problem prevents BDW theory from being widely used, that is, the integral is divergent at the exact boundary positions and leads to false results.

To solve this problem, in [15], Umul proposed the so-called uniform BDW theory by introducing a field parameter and provided a uniform expression of BDW integral for the case of semi-infinite half plane. In this paper, uniform BDW theory was used to solve the diffraction problem of multiple-disk occulters in external coronagraphs. The theory of BDW and uniform BDW theory were briefly introduced in Section 2, and an analytical propagator in single-disk diffraction case was approached using uniform BDW theory in Section 3 as a preparation; besides, the results were compared with Fresnel-Kirchoff integral method to prove the accuracy and efficiency. In Section 4, the case of multiple-disk diffraction was dealt with. The secondary diffraction wave was generated by non-planar diffraction field, which will result in an additional term called the gradient diffraction wave. We derived the expression of gradient diffraction wave and proved on numerical basis that its influence was too small to be included. Thus, we obtained an analytical propagator for multiple-disk diffraction by iterative utilization of the single-disk diffraction propagator.

2. Brief review of uniform BDW theory

In this section, the BDW diffraction theory and the improved version - uniform BDW theory will be briefly reviewed [15]. The BDW theory describes the diffraction wave field at observation point P as

$$\begin{cases} U(P) = U_G(P) + U_B(P), \ P \ in \ illuminated \ region \\ U(P) = U_B(P), \ P \ in \ shadow \ region \end{cases}, \tag{1}$$

where $U_G(P)$ refers to the geometrical propagation wave, and $U_B(P)$ represents the boundary wave. Considering a point source illuminating an aperture (shown in Fig. 1), the geometric propagation wave at point P can be expressed as a spherical wave,

$$U_G(P) = \frac{\exp(jkr)}{r}, \tag{2}$$

where k refers to the wave number and r represents the distance from the point source to the observation point. The boundary wave can be expressed as the following integral along the edge contour [16],

$$U_B(P) = \frac{1}{4\pi} \oint_C \frac{e^{jk(r_0+R_e)}}{r_0 R_e} \cdot \frac{\sin\alpha}{1-\cos\alpha} \cdot \sin(r_0, dl)dl, \tag{3}$$

In Eq. (3), r_0 refers to the distance from the point source to the aperture edge; R_e refers to the distance from the edge to the observation point P, and α represents the angle between the shadow boundary and the boundary wave from the edge to the observation point. From the mathematics point of view, the BDW expression is equivalent to Huygens principle due to the Stokes integral transformation. Nevertheless, when the observation point is located exactly at the shadow boundary, there will be $\alpha = 0$ and the integral will be infinite, leading to a false result.

Optics EXPRESS

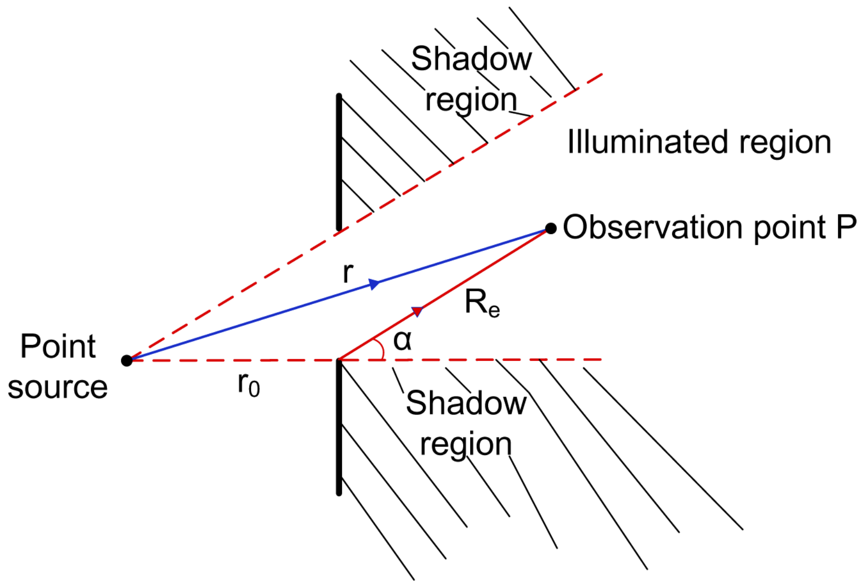

Fig. 1. Scheme of the diffraction of a point source by an aperture

The uniform BDW theory is proposed by introducing a new parameter [15]

$$V = \frac{\partial}{\partial k}[e^{-jkR_0} R_0 U_B(P)]. \tag{4}$$

In Eq. (4), R_0 has the value of $r_0 + R_e(\alpha = 0)$. Then the diffraction field can be expressed in an integral form,

$$U_B(P) = \frac{e^{jkR_0}}{R_0} \int_k^{\infty} V(\eta) d\eta. \tag{5}$$

Substituting (3) into (4), we obtain the expression of V as

$$V = \frac{jR_0}{4\pi} \int_C \frac{e^{jk(r_0+R_e-R_0)}}{r_0 R_e} \cdot \frac{(r_0 + R_e - R_0)\sin\alpha}{1 - \cos\alpha} \cdot \sin(r_0, dl) dl. \tag{6}$$

Suppose that the edge contour of C is continuous or the limits of the integral are infinity. Considering that there is only one exponential oscillating term in the integral, the stationary phase method is available for the approximate solution [16]. Denote the phase function as

$$g(l) = r_0 + R_e - R_0. \tag{7}$$

The stationary phase points locate at $g'(l) = 0$, denoted by l_s. Then near the stationary phase point we make a 2^{nd} order Taylor expansion and get

$$g(l) \approx g(l_s) + \frac{1}{2} g''(l_s) \cdot (l - l_s)^2. \tag{8}$$

Using this expansion, Eq. (6) can be also expanded near l_s,

$$V \approx \frac{jR_0}{4\pi} \cdot \frac{e^{jkg(l_s)}}{r_{0s} R_{es}} \cdot \frac{g(l_s) \cdot \sin\alpha_s}{1 - \cos\alpha_s} \cdot \sin(r_{0s}, dl_s) \int_{-\infty}^{\infty} e^{jk\frac{g''(l_s)}{2}(l-l_s)^2} dl, \tag{9}$$

where the subscript s denotes the value at l_s. If $g(l)$ has more than one stationary phase points within the integral limit, we should expand (6) at each point and the final result will be the sum.

Optics EXPRESS

The integral of Gaussian function on infinity intervals can be analytical expressed. Therefore, we get

$$V = \frac{e^{j\pi/4}R_0}{2\sqrt{2}\pi} \cdot \frac{e^{jkg(l_s)}}{r_{0s}R_{es}\sqrt{kg''(l_s)}} \cdot \frac{g(l_s)\cdot\sin\alpha_s}{1-\cos\alpha_s} \cdot \sin(r_{0s}, dl_s). \tag{10}$$

Substituting (10) into (5), we can obtain the diffraction field in the form of integral about the wavenumber k,

$$U_B(P) = \frac{e^{j\pi/4}\cdot e^{jkR_0}}{2\sqrt{2}\pi} \cdot \frac{g(l_s)}{r_{0s}R_{es}\sqrt{g''(l_s)}} \cdot \frac{\sin\alpha_s}{1-\cos\alpha_s} \cdot \sin(r_{0s}, dl_s) \cdot \int_k^\infty \frac{e^{j\eta g(l_s)}}{\sqrt{\eta}} d\eta. \tag{11}$$

The integral can be analytically expressed using Fresnel function after making a variable transformation as

$$\frac{\pi}{2}t^2 = \eta g(l_s), \tag{12}$$

and the integral is

$$\int_k^\infty \frac{e^{j\eta g(l_s)}}{\sqrt{\eta}} d\eta = \sqrt{\frac{2\pi}{g(l_s)}} \cdot \int_{\xi_s}^\infty e^{j\frac{\pi}{2}t^2} dt = \sqrt{\frac{2\pi}{g(l_s)}} \cdot [\frac{1}{2} - Fc(\xi_s) + \frac{1}{2}j - j\cdot Fs(\xi_s)], \tag{13}$$

where $\xi_s = \sqrt{\frac{2kg(l_s)}{\pi}}$. Fc and Fs denote the Fresnel cosine and sine functions respectively. Then we get the analytical expression of the diffraction field as

$$U_B(P) = \frac{e^{j\pi/4}\cdot e^{jkR_0}}{2\sqrt{\pi}} \cdot \frac{\sqrt{g(l_s)}\cdot\sin\alpha_s\cdot\sin(r_{0s}, dl_s)}{r_{0s}R_{es}\sqrt{g''(l_s)}\cdot(1-\cos\alpha_s)} \cdot [\frac{1}{2} - Fc(\xi_s) + \frac{1}{2}j - j\cdot Fs(\xi_s)]. \tag{14}$$

In the derivation process, the only assumption made is that the exponential term $e^{jkg(l)}$ is a fast oscillating term and the integral result is only related with the stationary phase point, which means $g(l)$ should be much larger than the wavelength. In the case that $g(l)$ is too small compared with the scale of the wavelength, the stationary phase approximation cannot be tenable and an alternative simplification should apply. In the next section, we will show this in specific conditions.

3. Diffraction by a single disk

The diffraction by a single disk presents a rather fundamental problem in physical optics. In this section, uniform BDW theory as above will be used to derive an analytical propagator, which is the basis of multiple-disk case. Fresnel-Kirchoff integral method has been proved to be available for good prediction in this case, therefore, it was employed as a comparing method to demonstrate the accuracy and efficiency of this propagator.

The scheme is shown in Fig. 2. Suppose the incident light is in parallel with the z-axis. The radius of the disk is R_b, and the observing plane is at $z = z_0$. The occulter is supposed to be totally absorptive and reflective so the incident field within the occulter's range is zero. For convenience in circular symmetric case, polar coordinate is utilized in this paper where the boundary point is denoted by $(R_b\cos\theta_0, R_b\sin\theta_0, 0)$ and the observing point P is $(r\cos\theta, r\sin\theta, z_0)$. Thanks to the circular symmetry, it is only needed to calculate the diffraction field along one direction. In that case, we suppose $\theta = 0$.

Here we express the parameters in the integral of Eq. (3) in vector form for convenience since the coordinate can be directly used and the need to calculate a series of angles is thus saved.

$$U_B(r) = \frac{1}{4\pi}\int \frac{e^{jkS}}{S} \cdot \frac{\vec{p}\times\vec{s}}{1-\vec{p}\cdot\vec{s}} \cdot d\vec{l}. \tag{15}$$

$\vec{p}$ represents the unit vector of the geometrically incident ray. The $\vec{p}$ vector is $(0, 0, 1)^T$ since the incident light is supposed to be along z-axis. S represents the distance from the source point at

Optics EXPRESS

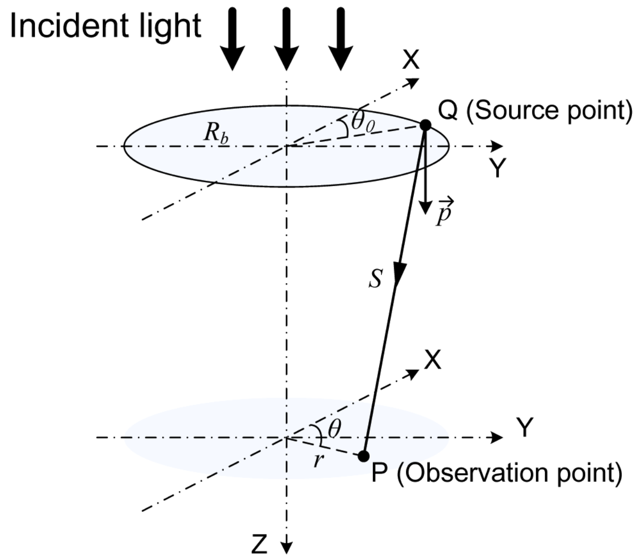

Fig. 2. Scheme of the diffraction of a single disk

the edge of the disk to the observation point, with $\vec{s}$ as the corresponding unit vector,

$$S = \sqrt{R_b^2 + r^2 - 2R_b r\cos\theta_0 + z_0^2},\ \vec{s} = \frac{1}{S}\begin{pmatrix} r - R_b\cos\theta_0 \\ 0 - R_b\sin\theta_0 \\ z_0 \end{pmatrix}. \tag{16}$$

The differential element $d\vec{l}$ can be expressed as

$$d\vec{l} = R_b \cdot d\theta_0 \cdot (\ \sin\theta_0, \quad -\cos\theta_0, \quad 0\ )^T. \tag{17}$$

Substituting (16) and (17) into (15), we obtain

$$U_B(r) = \frac{1}{4\pi}\int_0^{2\pi} \frac{e^{jkS}}{S} \cdot \frac{R_b(r\cos\theta_0 - R_b)}{S - z_0} d\theta_0. \tag{18}$$

Then the field parameter V given by Eq. (4) is

$$V = \frac{j}{4\pi}\int_0^{2\pi} \frac{e^{jk(S-z_0)}}{S} \cdot R_b(r\cos\theta_0 - R_b) d\theta_0. \tag{19}$$

The limit of the integral in (19) is not infinity, but stationary phase approximation is still available to be utilized here when extending the integral limit by the periodicity of cosine function, as what have been done in stellar coronagraphs [11]. The derivation of $S - z_0$ about θ_0 is expressed as:

$$\frac{\partial(S - z_0)}{\partial\theta_0} = \frac{R_b r\sin\theta_0}{S}. \tag{20}$$

The critical points are $\theta_0 = 0$ and $\theta_0 = \pi$, which are along the radial direction of the observation from the same side and the opposite side respectively. The second order derivations at these two

Optics EXPRESS

points are expressed as:

$$\begin{cases} \frac{\partial^2(S-z_0)}{\partial\theta_0^2} = \frac{R_b r}{S}, & \theta_0 = 0 \\ \frac{\partial^2(S-z_0)}{\partial\theta_0^2} = \frac{-R_b r}{S}, & \theta_0 = \pi \end{cases}. \tag{21}$$

Thus, the analytical solution of Eq. (19) under stationary phase approximation is obtained as:

$$V = \frac{j}{4\pi} e^{j\frac{\pi}{4}} e^{jkz_0} [\sqrt{\frac{2\pi S_1}{kR_b r}} \cdot \frac{R_b r - R_b^2}{S_1} \cdot e^{jkS_1} + \sqrt{\frac{-2\pi S_{-1}}{kR_b r}} \cdot \frac{R_b r + R_b^2}{S_{-1}} \cdot e^{jkS_{-1}}], \tag{22}$$

where

$$S_1 = \sqrt{z_0^2 + (R_b - r)^2}, S_{-1} = \sqrt{z_0^2 + (R_b + r)^2}. \tag{23}$$

Substituting (22) and (23) into (5), we can get the diffraction field in the form of integral about the wavenumber k

$$\begin{aligned} U_B(r) = \frac{je^{j\frac{\pi}{4}}}{4\pi} e^{jkz_0} \sqrt{\frac{2\pi}{R_b r}} \cdot [\int_k^\infty \sqrt{\frac{1}{\eta S_1}} \cdot \frac{R_b r - R_b^2}{S_1} \cdot e^{j\eta(S_1 - z_0)} d\eta \\ + \int_k^\infty \sqrt{\frac{-1}{\eta S_{-1}}} \cdot \frac{R_b r + R_b^2}{S_{-1}} \cdot e^{j\eta(S_{-1} - z_0)} d\eta] \end{aligned} \tag{24}$$

Using the same method in Section 2, the analytical expression of the integral in (24) can be obtained by means of Fresnel cosine and sine functions, that is,

$$\begin{aligned} \int_k^\infty \sqrt{\frac{1}{\eta S_1}} \cdot e^{j\eta(S_1 - z_0)} d\eta &= \sqrt{\frac{2\pi}{S_1 - z_0}} \cdot [\frac{1}{2} + \frac{1}{2}j - Fc(\sqrt{\frac{2k}{\pi}}(S_1 - z_0)) - j \cdot Fs(\sqrt{\frac{2k}{\pi}}(S_1 - z_0))] \\ &= \sqrt{\frac{2\pi}{S_1 - z_0}} I_1 \end{aligned} \tag{25}$$

and

$$\begin{aligned} \int_k^\infty \sqrt{\frac{1}{\eta S_{-1}}} \cdot e^{j\eta(S_{-1} - z_0)} d\eta &= \sqrt{\frac{2\pi}{S_{-1} - z_0}} \cdot [\frac{1}{2} + \frac{1}{2}j - Fc(\sqrt{\frac{2k}{\pi}}(S_{-1} - z_0)) - j \cdot Fs(\sqrt{\frac{2k}{\pi}}(S_{-1} - z_0))] \\ &= \sqrt{\frac{2\pi}{S_{-1} - z_0}} I_{-1} \end{aligned} \tag{26}$$

We hereby denote the expression as I_1 and I_{-1} for short. Substituting (25) and (26) into (24), the analytical expression of the diffraction field can be obtained as

$$U_B(r) = \frac{je^{j\frac{\pi}{4}}}{2\sqrt{R_b r}} e^{jkz_0} \cdot [\frac{R_b r - R_b^2}{\sqrt{S_1(S_1 - z_0)}} I_1 + \frac{R_b r + R_b^2}{\sqrt{S_{-1}(S_{-1} - z_0)}} I_{-1}]. \tag{27}$$

Equation (27) seems still to be singular at the edge when $r = R_b$, where $S_1 = z_0$ and $\frac{1}{\sqrt{S_1 - z_0}} \to \infty$. However, the term of $R_b r - R_b^2$ also equals to zero and their production is provided with a finite value. Denote the angle between $\vec{p}$ and $\vec{s}_1$ as β_1, and there is

$$|r - R_b| = S_1 \sin\beta_1, z = S_1 \cos\beta_1. \tag{28}$$

Then we will get

$$\frac{R_b r - R_b^2}{\sqrt{S_1(S_1 - z_0)}} = \pm \frac{R_b S_1 \sin\beta_1}{S_1\sqrt{1 - \cos\beta_1}} = \pm\sqrt{2} R_b \cos\frac{\beta_1}{2}. \tag{29}$$

Equation (29) is positive when $r \geq R_b$ and negative when $r < R_b$, which means discontinuity exists at the edge. This is logical and necessary since BDW theory defines the diffraction field in a

Optics EXPRESS

discontinuous form at the edge contour by adding a geometrical propagation term. Therefore, the BDW term should also be discontinuous at the edge to make the total diffraction field continuous. By means of the same simplification to the other stationary phase point, we have

$$\frac{R_b r + R_b^2}{\sqrt{S_{-1}(S_{-1} - z_0)}} = \sqrt{2} R_b \cos\frac{\beta_{-1}}{2}, \tag{30}$$

where β_1 refers to the angle between $\vec{p}$ and $\vec{s}_{-1}$. No sign marker is in Eq. (30) since R_b and r are always positive. Therefore, the diffraction field of a single disk can be analytically expressed as

$$U(r) = \begin{cases} \frac{je^{j\frac{\pi}{4}} e^{jkz_0}}{\sqrt{2R_b r}}[-R_b I_1 \cos\frac{\beta_1}{2} + R_b I_{-1} \cos\frac{\beta_{-1}}{2}], & r<R_b \\ \frac{je^{j\frac{\pi}{4}} e^{jkz_0}}{\sqrt{2R_b r}}[R_b I_1 \cos\frac{\beta_1}{2} + R_b I_{-1} \cos\frac{\beta_{-1}}{2}] + e^{jkz_0}, & r \geq R_b \end{cases}. \tag{31}$$

Unfortunately, singularity still exists in Eq. (31) at $r = 0$ due to the stationary phase approximation employed in the derivation. As stated in Section 2, when r is very small compared with the scale of wavelength, or in another word, when the field at the central point and neighboring positions are calculated, the stationary phase approximation cannot give good accordance without the characteristics of highly oscillating. In paraxial region, S can be expressed in Fresnel approximation as follows,

$$S = \sqrt{z_0^2 + r^2 + R_b^2 - 2R_b r\cos\theta_0} \approx z_0 + \frac{r^2 + R_b^2 - 2R_b r\cos\theta_0}{2z_0}. \tag{32}$$

To keep the stationary phase approximation tenable, there should be

$$\frac{kR_b r}{z_0} \gg 1, \tag{33}$$

or

$$r \gg \frac{z_0}{kR_b} = \frac{\lambda z_0}{2\pi R_b}. \tag{34}$$

Considering the scale of wavelength, this threshold is usually very small. As a comparison, the first zero-point of Arago spot is $\frac{1.53\lambda z_0}{2R_b}$, which is 4.8 times of this value. This means that the diffraction field at most points can be calculated by (31). However, in external solar coronagraphs, the radial sampling should be much tighter than Arago spot for the following calculation of propagation in the optical system based on Shannon's criteria [5]. In this case, we should date back to the original boundary wave integral Eq. (18). Since r is small, there will be $r\cos\theta_0 \ll R_b$ and Eq. (18) will be approximated as follows:

$$U_B(r) \approx \frac{1}{4\pi}\int_0^{2\pi} \frac{e^{jkS}}{S} \cdot \frac{-R_b^2}{S - z_0} d\theta_0. \tag{35}$$

Using Fresnel approximation to S, (35) can be further simplified as

$$\begin{aligned} U_B(r) &\approx -\frac{1}{2\pi} e^{jkz_0} e^{jk\frac{r^2+R_b^2}{2z_0}} \int_0^{2\pi} e^{-j\frac{krR_b}{z_0}\cos\theta_0} d\theta_0 \\ &= -\frac{1}{2\pi} e^{jkz_0} e^{jk\frac{r^2+R_b^2}{2z_0}} J_0(\frac{krR_b}{z_0}), \end{aligned} \tag{36}$$

where $J_0(x)$ is the 1st class Bessel function, and Eq. (36) is also an analytical expression in a very clear form. It is available to artificially definite a boundary, at which Eq. (36) is used for smaller

r and Eq. (31) is used for larger r. Typically, for example, we can just choose the zero-point of Arago spot as the boundary. Finally, so far, we obtain the analytical solution for the diffraction by means of a single disk based on uniform BDW theory

$$U(r)=\begin{cases} -\frac{1}{2\pi}e^{jkz_0}e^{jk\frac{r^2+R_b^2}{2z_0}}J_0(\frac{krR_b}{z_0}), & r<\frac{1.53\lambda z_0}{2R_b} \\ \frac{je^{j\frac{\pi}{4}}e^{jkz_0}}{\sqrt{2R_b r}}[-R_bI_1\cos\frac{\beta_1}{2}+R_bI_{-1}\cos\frac{\beta_{-1}}{2}], & \frac{1.53\lambda z_0}{2R_b}\le r<R_b \\ \frac{je^{j\frac{\pi}{4}}e^{jkz_0}}{\sqrt{2R_b r}}[R_bI_1\cos\frac{\beta_1}{2}+R_bI_{-1}\cos\frac{\beta_{-1}}{2}]+e^{jkz_0}, & r\ge R_b \end{cases}. \tag{37}$$

From the mathematics point of view, this propagator is not perfect due to the fact that it induces discontinuity to the diffraction field at the zero-point of Arago spot. However, in practice, it is available to present accurate results if only the diffraction field at discrete positions is concerned.

Equation (37) is derived in the case that the incident light propagates along the z-axis. In the case of off-axis, the diffraction field is the lateral shift compared to the on-axis light, as proved in [6]. Suppose the incident light is at the tilt angle of (α,β) with x-axis and y-axis respectively, the diffraction field is described by

$$U(x,y,\alpha,\beta)=e^{-jk(\alpha x+\beta y)}e^{-j\frac{kz_0}{2}(\alpha^2+\beta^2)}U(x+z_0\tan\alpha,y+z_0\tan\beta,0,0). \tag{38}$$

The holding condition of the propagator is discussed here since during the derivation process, two approximations have been used. The first one is the stationary phase approximation to the uniform BDW integral Eq. (19). The holding condition is that the integrand is exponentially fast oscillating within the integration range as expressed in Eq. (33). In another word, this propagator is more appropriate for high Fresnel number systems. For example, if we want the approximation is valid at $r>R_b/1000$, the Fresnel number should be much larger than 160. Actually, it is an easily satisfied condition for actual coronagraph systems (usually much higher than 1000). The second approximation is the Fresnel approximation, employed in the derivation of the central region field, and the holding condition is the same as used in Huygens-Fresnel principle.

A numerical demonstration was implemented to prove the accuracy of the analytical propagator, and the results were compared with those obtained with Fresnel-Kirchoff integral method. Here, the design of solar coronagraph ASPIICS was used, given in [5] since it is most close to the actual usage. The radius of the external occulter is $R_b = 710$mm, and the distance between the occulter to the entrance pupil is $z_0 = 144.348$m. Besides, the wavelength is 550 nm, corresponding to the Fresnel number of 6349.5. Other parameters of the optical system are left unused in this paper when only the diffraction was calculated with the external occulter.

Fresnel-Kirchoff theory provides the solution of circular diffraction in a radial Hankel transformation term [6],

$$U(r)=1-\frac{e^{j\lambda z_0}e^{j\frac{kr^2}{2z}}}{j\lambda z_0}\int_0^R 2\pi\rho\cdot e^{j\frac{k\rho^2}{2z}}\cdot J_0(\frac{k\rho r}{z})\cdot d\rho. \tag{39}$$

The integral was analytically calculated with the sum of Lommel series. 50 terms were used in general regions while 2000 terms were used near the shadow boundary due to the much slower convergence of Lommel series at this region. In the radial direction, 10^5 discrete points were sampled between $r = 0$ to $1.2R_b$. The field intensity based on the two propagators and their differences in logarithmic scale was shown in Fig. 3, and the two results matched perfectly. In the shadow region, the differences were typically below 10^{-5} scale while the actual intensities were $10^{-3}\sim10^{-4}$, while in the illuminated region, the field intensity was oscillating around 1 and the differences were at 10^{-3} scale. Nevertheless, the difference near the shadow boundary is still obviously higher than that of other regions (shown in Fig. 3(c)). Therefore, we numerically calculated the Fresnel-Kirchoff integral by adaptive Gauss-Kronrod (15^{th} and 7^{th} order formulas)

Optics EXPRESS

method. The calculation results and the difference with uniform BDW theory were showed in Fig. 3(d), which showed better accuracy and no divergence at the transition between shadow and illuminated regions. This indicates that the difference in Fig. 3(c) was mainly caused by the cut-off error of Lommel series, not the uniform BDW theory (We tried to increase the order to 10000 but the "peak" of the difference still exists). The convergence at the transition point proved the most important improvement of uniform BDW theory compared with the traditional BDW theory.

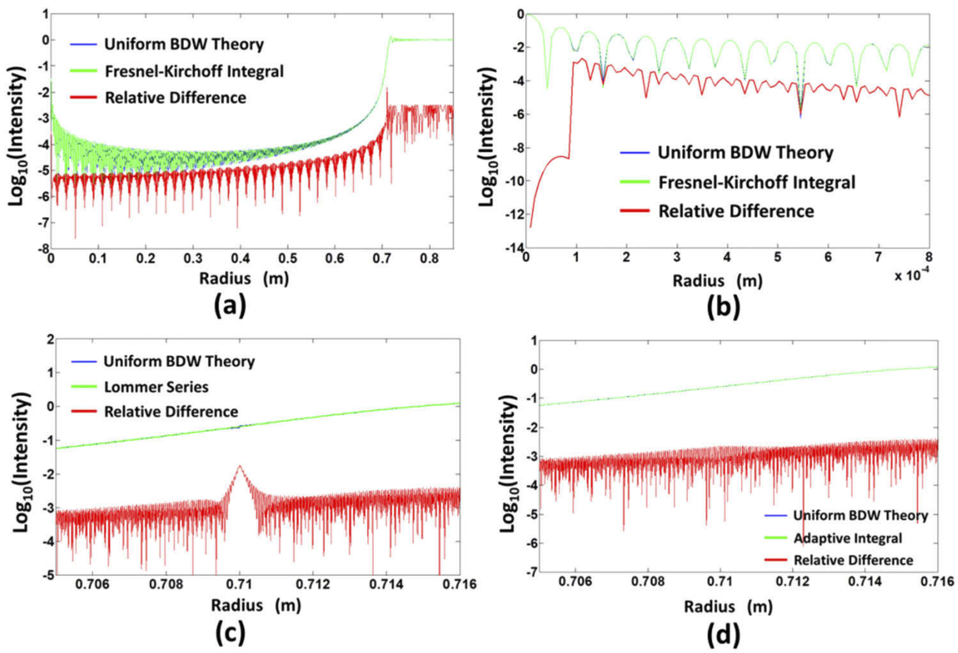

Fig. 3. The diffraction fields calculated by the analytical propagator of uniform BDW theory and Fresnel-Kirchoff integral method. Panel a: full range, in logarithmic scale. Panel b: zoom in the Arago bright spot in the central region, in logarithmic scale. Panel c: zoom in the transition region around the edge, in logarithmic scale. Panel d: comparison of the results given by uniform BDW theory and adaptive numerical solution of Fresnel-Kirchoff integral in the transition region

In the central region showed in Fig. 3(b), the relative difference within the Arago spot, which is calculated by Fresnel approximation of original BDW integral, is obviously smaller, than the outer region, which is calculated by the propagator given by uniform BDW theory. Nevertheless, no matter which propagator, the relative difference to Fresnel-Kirchhoff integral is below 10^{-3}, which shows good accordance.

Although a little less convenient, the propagator within the Arago spot is a necessary supplement to the final analytical propagator since the telescope is usually located at the center in coronagraphs. However, the Arago spot of external occulters is usually small and make the influence actually small. Take the design of solar coronagraph ASPIICS as an example, the radius of Arago spot at 550 nm wavelength is 0.085mm, compared to the 25mm radius entrance pupil. That means most of the diffraction fields will be calculated by the uniform BDW propagator. In stellar coronagraphs, the Fresnel number will be much higher than that of solar coronagraphs since the inner working angle is only the scale of 0.01~0.1 arcsec, which will make the Arago spot even smaller.

In the premise of good accuracy, when comparing the calculation efficiency, the uniform BDW theory still shows higher calculation efficiency, although both propagators are analytical. It takes about 4 minutes to calculate 10^5 points using Lommel series solution of Fresnel-Kirchoff integral on a general PC, while the same calculation by BDW propagator only needs about 1.5 minutes, which is faster by more than 2 times. It is easy to understand since the calculation of high order Lommel series near the boundary is more time-consuming.

In Fig. 4, the contribution of the two stationary phase points was shown respectively. The diffraction field induced by $\theta_0 = 0$ showed the highest values near the shadow boundary, and decreased rapidly when the observation points got far away. The opposite side stationary phase point should follow the same tendency. Therefore, the two diffraction fields were of almost the same scale near the central region, while the contribution of the same side stationary phase point was 2~5 orders higher when r was larger. Near the boundary region, the diffraction field was almost totally induced by $\theta_0 = 0$.

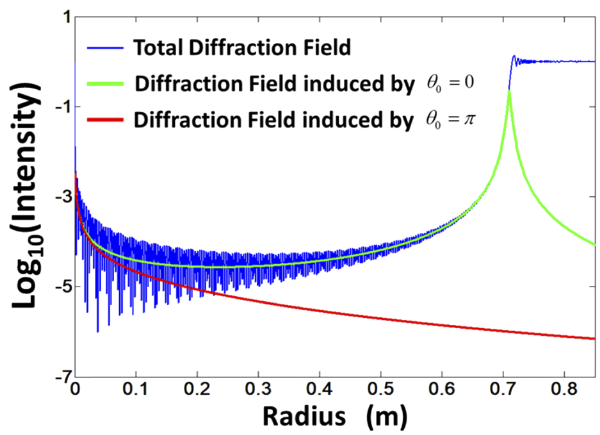

Fig. 4. Diffraction fields induced by the two stationary phase points

4. Diffraction by multiple-disk occulter

The propagator for multiple-disk diffraction based on the analytical propagator for single disk diffraction will be proposed in this section. The classical three-disk occulter was used as an example, and the scheme was shown in Fig. 5. The second disk is located in the shadow region of the first disk, and the third disk is in the shadow of the second one. Therefore, the following disks will diffract the light for one more time and hence lower the energy projected to the entrance pupil plane. In practice, the radius of the sun disk should be considered, however, in this paper, we maintain the assumption that the incident light is along the z-axis as what we did in Section 3, and hence the scheme is still circular asymmetric. The radius of the three disks are denoted by R_1, R_2 and R_3 respectively, and the distance between the disks is denoted by d. The observation point is located at the entrance pupil plane of the coronagraph with the coordinate of $z = z_0$; besides, α_1, α_2 and α_3 are the occulting angles of the disks, which represent the angle between the shadow boundary and the connection line of the disk edge.

The propagation process in the case of three-disk can be regarded as three successive diffractions, which propagate from disk-1 to disk-2, from disk-2 to disk-3 and from disk-3 to the entrance pupil plane of the coronagraph. The diffraction field at disk-2 plane can be accurately calculated using Eq. (37). However, the calculation of the second and third diffractions is more complicated since the incident light at disk-2 and disk-3 plane is a non-planar wave in the illuminated region. According to the extension theory of BDW raised by Suzuki [17], when the incident light is not a

Optics EXPRESS

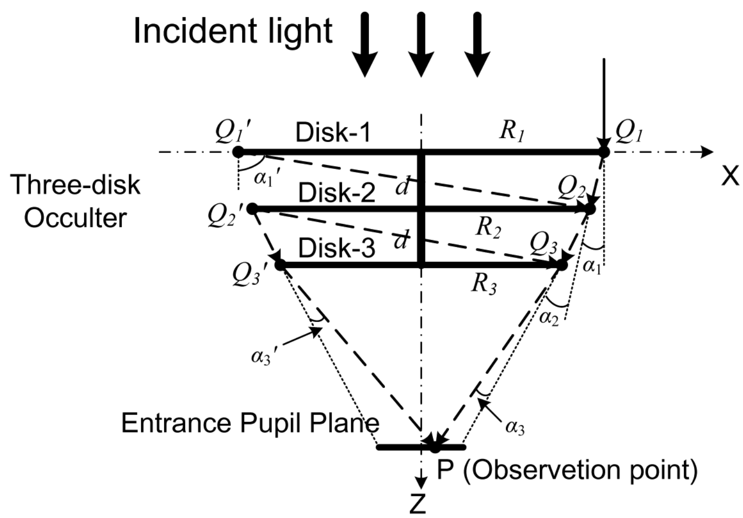

Fig. 5. Scheme of the diffraction of a three-disk occulter

planar wave, every point where the gradient is not zero will be the origin of a secondary wave besides the BDW and geometrical wave. This diffraction wave contributes another term in the expression of the diffraction field, which is called gradient diffraction wave.

Anyhow, the boundary diffraction term will be derived first. Using BDW theory as diffraction propagator, no matter in scalar form (See Eq. (3)) or vector form (See Eq. (15)), and the direction of the incident light needs to be determined as a precondition. As per BDW theory, in the shadow region, the diffraction field is caused by the edge of the occulter and the main contribution is from the two stationary phase points. Referring to the edge point at disk-2 $Q_2(R_2, 0, d)$, the stationary phase points at the edge of disk-1 are denoted by $Q_1(R_1, 0, 0)$ and $Q_1'(-R_1, 0, 0)$ respectively. We hereby define

$$U_{Q_1Q_2} = \frac{-je^{j\frac{\pi}{4}}e^{jkd}}{\sqrt{2R_1R_2}}R_1\cos\frac{\alpha_1}{2}[\frac{1}{2}+\frac{1}{2}j - Fc(\sqrt{\frac{2k}{\pi}}(S_{Q_1Q_2}-d)) - j\cdot Fs(\sqrt{\frac{2k}{\pi}}(S_{Q_1Q_2}-d))], \quad (40)$$

and

$$U_{Q'_1Q_2} = \frac{je^{j\frac{\pi}{4}}e^{jkd}}{\sqrt{2R_1R_2}}R_1\cos\frac{\alpha_1'}{2}[\frac{1}{2}+\frac{1}{2}j - Fc(\sqrt{\frac{2k}{\pi}}(S_{Q'_1Q_2}-d)) - j\cdot Fs(\sqrt{\frac{2k}{\pi}}(S_{Q'_1Q_2}-d))], \quad (41)$$

to represent the two fields propagated from Q_1 and Q_1'. Then the diffraction field at Q_2 is expressed as:

$$U_B(Q_2) = U_{Q_1Q_2} + U_{Q'_1Q_2}. \quad (42)$$

As demonstrated in Section 3, near the shadow boundary, the contribution of the opposite side stationary phase point is much smaller than that of the same side one. Therefore, we make the approximation that

$$U_B(Q_2) \approx U_{Q_1Q_2}, \quad (43)$$

and hence the diffraction light at Q_2 propagates along the orientation of QQ_1. In another word, the diffraction light at the edge point of disk-2 propagates from the corresponding stationary phase point at the same side of disk-1.

The BDW field at the edge of disk-3 can be calculated at given direction of incident ray. Unfortunately, Eq. (37) cannot be directly used here since the incident light is in different

Optics EXPRESS

orientations at different edge points. Therefore, we should go back to the vector form of the BDW integral Eq. (15).

The coordinate of the edge point Q_3 at disk-3 is $(R_3, 0, 2d)$, and the source point at the edge of disk-2 is denoted by $(R_2\cos\theta_2, R_2\sin\theta_2, d)$. The unit vector of the incident ray is expressed as:

$$\vec{p} = (\sin\alpha_1\cos\theta_2, \sin\alpha_1\sin\theta_2, \cos\alpha_1)^T. \tag{44}$$

The propagation vector from the source point to the observation point is expressed as:

$$\vec{s} = \frac{1}{S}\begin{pmatrix} R_3 - R_2\cos\theta_2 \\ 0 - R_2\sin\theta_2 \\ d \end{pmatrix}, \; S = \sqrt{R_2^2 + R_3^2 - 2R_2R_3\cos\theta_2 + d^2}. \tag{45}$$

The differential element $\vec{dl}$ can be expressed as

$$\vec{dl} = R_2 \cdot d\theta_2 \cdot (\;\sin\theta_2, \quad -\cos\theta_2, \quad 0\;)^T. \tag{46}$$

Substituting (44) ~ (46) into (15), we obtain

$$U_B(Q_3) = \frac{U_B(Q_2)}{4\pi}\int_0^{2\pi}\frac{e^{jkS}}{S}\cdot\frac{R_2 d\sin\alpha_1 + R_2^2\cos\alpha_1 - R_2R_3\cos\theta_2\cos\alpha_1}{S - d\cos\alpha_1 + R_2\sin\alpha_1 - R_3\sin\alpha_1\cos\theta_2}d\theta_2. \tag{47}$$

Despite of the fact that the expression seems more complicated, the following procedure is exactly the same as what we did in Section 3, except that we neglect the opposite side stationary phase point Q_2'. We hereby give the final result only as follows:

$$U_B(Q_3) = U_B(Q_2)\cdot\frac{-je^{j\frac{\pi}{4}}e^{jk[d\cos\alpha_1+(R_3-R_2)\sin\alpha_1]}}{\sqrt{2R_2R_3}}R_2\cos\frac{\alpha_2}{2}[\frac{1}{2}+\frac{1}{2}j - Fc(\xi_1) - j\cdot Fs(\xi_1)], \tag{48}$$

where

$$\xi_1 = \{\frac{2k}{\pi}[\sqrt{d^2 + (R_3 - R_2)^2} - d\cos\alpha_1 - (R_3 - R_2)\sin\alpha_1]\}^{1/2}. \tag{49}$$

Compared with the normal incidence case, the only difference in Eq. (48) is the substitution of the vertical distance d with a tilt factor $d\cos\alpha_1 + (R_3 - R_2)\sin\alpha_1$.

Now we turn to the gradient diffraction wave term. To make it simple, we directly use the conclusion of Suzuki (Eq. (13) and (14) in [17]). The gradient diffraction wave can be expressed as

$$U_T(Q_3) = \frac{1}{4\pi}\iint(\nabla U_2(r)\times\vec{w})\cdot\vec{n}dS_I, \tag{50}$$

where S_I refers to the input aperture surface, or the illuminated region at disk-2 plane in another word, and $\vec{n}$ refers to the normal vector of S_I. $U_2(r)$ represents the diffraction field at disk-2 plane, and $\vec{w}$ refers to the vector form integrand in Eq. (15)

$$\vec{w} = \frac{e^{jkS}}{S}\cdot\frac{\vec{p}\times\vec{s}}{1-\vec{p}\cdot\vec{s}}, \tag{51}$$

where all parameters are defined in the same way. Denote the coordinate of the source point as $(r_2\cos\theta_2, r_2\sin\theta_2, d)$, then we get the expression of the parameters as follows:

$$\vec{p} = \begin{pmatrix} \sin\alpha_1\cos\theta_2 \\ \sin\alpha_1\sin\theta_2 \\ \cos\alpha_1 \end{pmatrix}, \; \vec{s} = \frac{1}{S}\begin{pmatrix} R_3 - r_2\cos\theta_2 \\ 0 - r_2\sin\theta_2 \\ d \end{pmatrix}, \; S = \sqrt{r_2^2 + R_3^2 - 2r_2R_3\cos\theta_2 + d^2}. \tag{52}$$

Optics EXPRESS

$U_2(r_2)$ refers to a circular symmetric function, therefore, the gradient is along the radial direction. Denote that

$$\nabla U_2(r_2) = U_2'(r_2) \cdot (\cos\theta_2, \sin\theta_2, 0)^T, \tag{53}$$

and then the scalar form of (50) can be obtained as:

$$U_T(Q_3) = \frac{1}{4\pi} \int_{R_2}^{R_o} \int_{0}^{2\pi} \frac{e^{jkS}}{S} \cdot \frac{(R_3\cos\theta_2 - r_2)\cos\alpha_1 - d\sin\alpha_1}{S - d\cos\alpha_1 - (R_3\cos\theta_2 - r_2)\sin\alpha_1} \cdot U'_2(r_2) r_2 dr_2 d\theta_2, \tag{54}$$

where R_o represents the outside radius of the input aperture. Equation (54) has to be further simplified due to the fact that it is difficult to implement numerical calculation against the 2D oscillating integral. The integration about θ_2 is similar to the BDW integral, and stationary phase approximation can be employed to simplify the 2D integral to 1D. Similar to the derivation in Section 3, the stationary phase points are $\theta_2 = 0$ and $\theta_2 = \pi$. Then we get

$$\begin{aligned} U_T(Q_3) = \frac{1}{4\pi} \int_{R_2}^{R_o} \sqrt{\frac{\lambda}{r_2 R_3}} \Bigg\{ & \frac{[(R_3 - r_2)\cos\alpha_1 - d\sin\alpha_1] e^{jkS_{23}}}{\sqrt{S_{23}}[S_{23} - d\cos\alpha_1 - (R_3 - r_2)\sin\alpha_1]} \\ & + \frac{j[(R_3 + r_2)\cos\alpha_1 + d\sin\alpha_1] e^{jkS_{-23}}}{\sqrt{S_{-23}}[S_{-23} - d\cos\alpha_1 + (R_3 + r_2)\sin\alpha_1]} \Bigg\} \cdot U'_2(r_2) \cdot r_2 \cdot dr_2, \end{aligned} \tag{55}$$

where

$$S_{23} = \sqrt{d^2 + (R_3 - r_2)^2}, S_{-23} = \sqrt{d^2 + (R_3 + r_2)^2}. \tag{56}$$

In Eq. (55), the stationary phase method is not directly available to determine the integral about r_2 on an analytical basis due to the fact that $U_2'(r_2)$ is also a highly oscillating function along the radial direction based on the Fresnel function in $U_2(r_2)$. Considering the specific expression of the derivation of the Fresnel function,

$$\frac{\partial[Fc(r_2) + jFs(r_2)]}{\partial r_2} = \frac{\partial}{\partial r_2} \int_0^{r_2} e^{j\frac{\pi}{2}\left(\sqrt{\frac{2k}{\pi}(S_{Q1r2} - d)}\right)^2} dr_2 = e^{jk(S_{Q1r2} - d)} \tag{57}$$

is also an exponential term, the integrand in Eq. (55) only has exponential oscillating term

$$e^{jk(S_{23} + S_{Q1r2})}, e^{jk(S_{-23} + S_{Q1r2})} \tag{58}$$

and the condition for using stationary phase approximation to evaluate the integration is meet. The derivations of the phase term are

$$\frac{\partial(S_{23} + S_{Q_1Q_2})}{\partial r_2} = \frac{r_2 - R_3}{S_{23}} + \frac{r_2 - R_1}{S_{Q1r2}}, \frac{\partial(S_{-23} + S_{Q_1Q_2})}{\partial r_2} = \frac{r_2 + R_3}{S_{-23}} + \frac{r_2 - R_1}{S_{Q1r2}}, \tag{59}$$

and the stationary phase points of the two derivations are

$$r_{s1} = \frac{R_1 + R_3}{2}, r_{s2} = \frac{R_1 - R_3}{2} \tag{60}$$

respectively. Both stationary phase points are smaller than R_2, which is beyond the integration interval. For the points on the third disk with $r<R_3$, the stationary phase point will be even smaller which is also beyond the integration interval. Therefore, under stationary phase approximation the integration result will be zero. In actual case, the integration will certainly not be exactly zero but we can make the inference that the value of the gradient diffraction field is very small, and can be neglected in the following calculation.

Optics EXPRESS

A numerical example was made to prove this inference, and similar parameters were used for better comparison, as in Section 3. The radius of disk-1 is R_1 = 865mm, the distance between the disks is d = 50mm, and the occulting angles are supposed to be α_1 = 18 arcmin,α_2 = 20 arcmin and α_3 = 22 arcmin respectively. The radius of disk-1 is larger than that of Section 3 since the three-disk design is with a larger occulting angle. The integration (55) was calculated by by adaptive Gauss-Kronrod (15$^{\text{th}}$ and 7$^{\text{th}}$ order formulas) method due to its high efficiency on the quadrature of oscillating integrands. The radius of following disks can be calculated according to the geometrical relationship shown in Fig. 5. The distance between the occulter to the entrance pupil is also supposed to be the same value, i.e., z_0 = 144.348m, and the outside radius of the aperture is R_o = 1300mm, which is supposed to be 1.5 times more than the occulter. Figure 6 shows the results of the BDW field and gradient diffraction field at disk-3 plane in logarithm scale. Being more than the edge point Q_3 and at the whole plane actually, the gradient diffraction field is 10^{-6} ∼10^{-3}(at the boundary) smaller than the BDW field, which means that in the diffraction propagation from disk-2 to disk-3, the total diffraction field is determined by BDW (as shown in Eq. (48)) and the gradient diffraction term can be neglected.

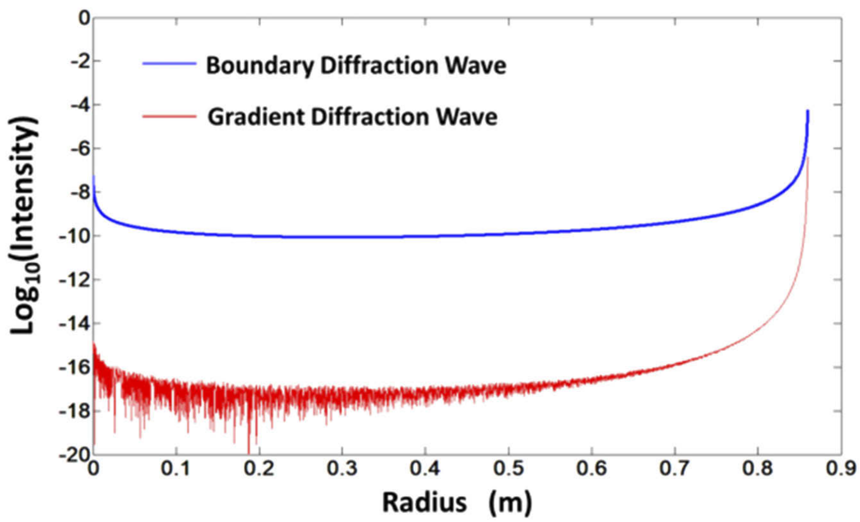

Fig. 6. Comparison of BDW field and gradient diffraction field at disk-3 (in logarithm scale)

With $U(Q_3)$ known, diffraction from disk-3 to the entrance pupil plane for the third time is easy to be known using similar method as above. Different from Eq. (48), the opposite side stationary phase point should also be considered for higher accuracy. In the range of

$$\frac{1.53\lambda(z_0-2d)}{2R_3} \leq r<R_3-(z_0-2d)\tan\alpha_3, \tag{61}$$

which means that in the shadow region and far from the center, the diffraction field is

$$U(r) = U_B(Q_3)\cdot\frac{je^{j\frac{\pi}{4}}}{\sqrt{2rR_3}}R_3[-e^{jkz'}\cos\frac{\alpha_3}{2}I_1+e^{jkz'}\cos\frac{\alpha'_3}{2}I_{-1}], \tag{62}$$

where

$$z' = (z_0-2d)\cos\alpha_2+(r-R_3)\sin\alpha_2, \tag{63}$$

$$I_1 = \frac{1}{2}+\frac{1}{2}j-Fc(\xi_1)-j\cdot Fs(\xi_1), \tag{64}$$

$$I_{-1} = \frac{1}{2} + \frac{1}{2}j - Fc(\xi_{-1}) - j \cdot Fs(\xi_{-1}), \tag{65}$$

$$\xi_1 = \{\frac{2k}{\pi}[\sqrt{(z_0-2d)^2+(r-R_3)^2} - (z_0-2d)\cos\alpha_2 - (r-R_3)\sin\alpha_2]\}^{1/2}, \tag{66}$$

$$\xi_{-1} = \{\frac{2k}{\pi}[\sqrt{(z_0-2d)^2+(r+R_3)^2} - (z_0-2d)\cos\alpha_2 - (r-R_3)\sin\alpha_2]\}^{1/2}. \tag{67}$$

In the derivation of $U(Q_3)$, the divergence near the central point is not considered since only the diffraction field at the edge is concerned for the following calculation. However, at the whole entrance pupil plane, the central point is also important for evaluating the occulting effects. Similar as Section 3, Fresnel approximation is also employed to S in the original BDW integral expression (Eq. (47) with the symbols changed) and an analytical propagator is obtained with Bessel function.

$$\begin{aligned}
U(r) &= \frac{U_B(Q_3)}{4\pi}\int_0^{2\pi}\frac{e^{jkS}}{S}\cdot\frac{(z_0-2d)R_3\sin\alpha_2 - R_3^2\cos\alpha_2 - rR_3\cos\theta_3\cos\alpha_2}{S-(z_0-2d)\cos\alpha_2 + R_3\sin\alpha_2 - r\sin\alpha_2\cos\theta_3}d\theta_3 \\
&\approx \frac{U_B(Q_3)}{4\pi}\int_0^{2\pi} e^{jk(z_0-2d)}e^{jk\frac{r^2+R_3^2}{2(z_0-2d)}}e^{-jk\frac{krR_3}{z_0-2d}\cos\theta_3}\cdot\frac{(z_0-2d)R_3\sin\alpha_2 - R_3^2\cos\alpha_2}{S[S-(z_0-2d)\cos\alpha_2 + R_3\sin\alpha_2]}d\theta_3 \\
&\approx \frac{U_B(Q_3)}{2\pi}e^{jk(z_0-2d)}e^{jk\frac{r^2+R_3^2}{2(z_0-2d)}}J_0(\frac{krR_3}{z_0-2d})\cdot\frac{(z_0-2d)\sin\alpha_2 - R_3\cos\alpha_2}{R_3}
\end{aligned} \tag{68}$$

The first order approximation about α_2 is also used here. Equation (68) is similar to the normal incidence expression Eq. (37) except for an additional coefficient containing the tilt factor α_2. Eventually, the analytical solution of the diffraction by a three-disk occulter based on uniform BDW theory is obtained.

$$U(r) = \begin{cases} \frac{U_B(Q_3)}{2\pi}e^{jk(z_0-2d)}e^{jk\frac{r^2+R_3^2}{2(z_0-2d)}}J_0(\frac{krR_3}{z_0-2d})\cdot\frac{(z_0-2d)\sin\alpha_2 - R_3\cos\alpha_2}{R_3}, & r<\frac{1.53\lambda(z_0-2d)}{2R_3} \\ U_B(Q_3)\cdot\frac{je^{j\frac{\pi}{4}}}{\sqrt{2rR_3}}R_3[-e^{jkz'}\cos\frac{\alpha_3}{2}I_1 + e^{jkz'}\cos\frac{\alpha'_3}{2}I_{-1}], & \frac{1.53\lambda(z_0-2d)}{2R_3}\le r<R_3-(z_0-2d)\tan\alpha_3 \end{cases}. \tag{69}$$

where z', I_1 and I_{-1} are defined in Eq. (63)–(67), and $U_B(Q_3)$ can be analytically determined by Eq. (40),(43),(48). For multiple-disk occulters with more than 3 disks, the propagator Eq. (68) is also applicable when $U_B(Q_3)$ is changed by $U_B(Q_n)$ and Eq. (48) is iteratively used to calculate the propagation from $U_B(Q_{n-1})$ to $U_B(Q_n)$. Although the derivation process is more complicated, the propagator in multiple-disk case is just the iterative utilization of the propagator (36) with an additional tilt factor when the gradient diffraction wave is neglected actually. As to the holding condition, the only additional approximation than that of (36) is the stationary phase approximation used in the prove of neglecting the gradient term. So the holding condition for this inference is the same as that of stationary phase approximation, as we stated in Section 3, high Fresnel number system like coronagraphs satisfies the holding condition.

The numerical results with this propagator are shown in Fig. 7. As a comparison, the result of single-disk is plotted with the same radius. Both results show similar distribution along the radial direction, this is because that the propagators are in similar form except for the tilt factor. The field intensity of three-disk occulter is lower than that of a single-disk occulter by$10^1\sim10^2$, and the decreasing extent is in accordance with the former experience [8]. From the calculation efficiency point of view, the time consumed by Eq. (68) is not more than that for the single-disk case, since 2 more points, i.e., Q_2 and Q_3 are calculated. In the case that Fresnel-Kirchoff integral is used to analyze the three-disk diffraction, the calculation of the radial Hankel transformation has to be repeated for three times while Lommel series cannot be used in the following diffraction of non-uniform incident field, which will be much more time-consuming.

To prove the validation of the propagator, we compared it to the solution given by Fresnel-Kirchoff integral. Applying Fresnel-Kirchoff integral to the on-axis diffraction problem of

Optics EXPRESS

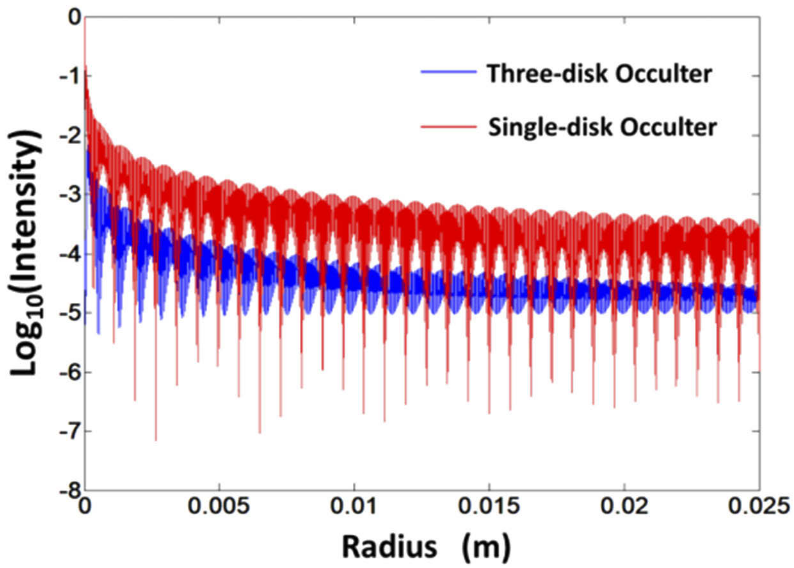

Fig. 7. Field intensity at the entrance pupil by single-disk and three-disk occulters

two-disk system has been successfully demonstrated in [7]. An example of two-disk system is employed here, which is sufficient for demonstrating the accuracy of the propagator for the secondary diffraction, since the third diffraction in 3-disk system is just one more time use of the propagator. The 3-disk system parameters of ASPIICS coronagraph used in this section indicates a large Fresnel number of over 27 million, which will cost tremendous time to calculate the Fresnel-Kirchoff integral. For simplification, we employ similar scheme and parameters with [7]. The radius of the two disks are assumed to be 2 mm and 1.5 mm respectively, the distance between the two disk and the second disk to the observation plane are equally 100 mm, indicating the shadow boundary at the observation plane is at the radius of 1 mm. The working wavelength is still assumed to be 550 nm. The Fresnel numbers of the two diffraction process are 72.7 and 40.9. Both the stationary phase approximation and Fresnel approximation are usable under this condition. Since the Fresnel number is not very large, we just made numerical sum of discrete samplings to calculate the Fresnel-Kirchoff integral of the secondary diffraction with a sampling distance of 10 nm (1/50 wavelength) while the field of the first diffraction was given by sum of Lommel series. When using uniform BDW theory, the contribution of the opposite side stationary phase point is also included as we did in the diffraction from disk-3 to the entrance pupil in three-disk system above. The diffraction field in the shadow region given by the two propagators and their differences in logarithmic scale was shown in Fig. 8, and the two results showed good accordance. The difference is usually below 10^{-3} while the diffraction field is at the level of 10^{-2} to 10^{-3}. The relative difference has a slightly increasing tendency near the boundary location to at most ~30%. An interesting and puzzled phenomenon is that the obvious higher relative difference compared to the case of single-disk is not due to the difference of the field intensity, but indeed the axial position of the "peak" and "valley" of the two results has a difference of ~5 µm or so. This is probably owing to the different approximations which will be deeply explored further in the future. Another possible reason is that the stationary phase approximation needs a highly oscillating exponential phase term, corresponding to a high Fresnel number and the small Fresnel number system in this example weakens the performance. Anyhow, the tiny difference of the axial position and field intensity at this scale will actually not influence the application on coronagraphs where we only care the scale of the diffraction field. On the

Optics EXPRESS

other hand, comparing the calculation efficiency, the uniform BDW theory is no doubt better than the Fresnel-Kirchoff integral. On a normal PC, in this example with only Fresnel number less than 100, calculating 2000 points using the Fresnel-Kirchoff integral of the secondary diffraction cost about 3 minutes, while the uniform BDW theory finished the calculation within 1 second.

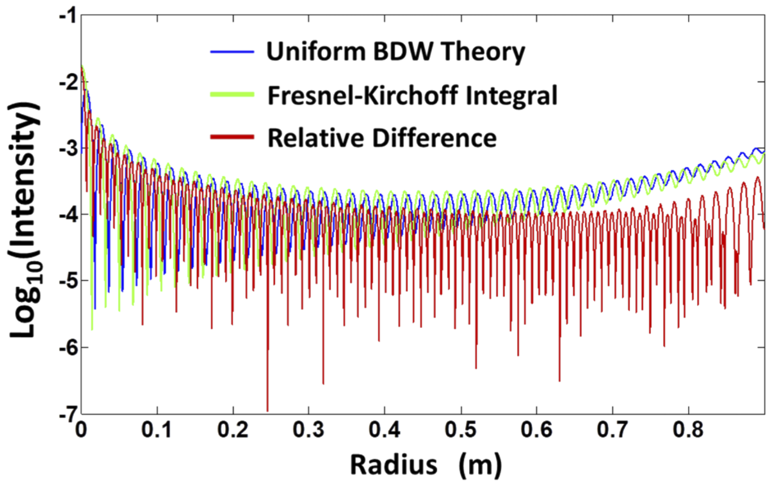

Fig. 8. The diffraction fields of a two-disk system calculated by the analytical propagator of uniform BDW theory and Fresnel-Kirchoff integral method.

5. Summary

In conclusion, an analytical propagator Eq. (68) is proposed in this paper for the diffraction analysis of multiple-disk occulters in external coronagraphs based on uniform BDW theory. The case of single-disk is first analyzed and an analytical propagator was obtained. This propagator is available to avoid the divergence of original BDW theory at the exact edge. Although a discontinuity is induced at the zero-point of Arago spot, the propagator is proved to have good accuracy compared with the results from Fresnel-Kirchoff integral in a numerical example. It is also verified by this numerical example that the analytical propagator was slightly more efficient than Fresnel-Kirchoff integral, compared to the well-known analytical propagator based on Lommel series. The propagator in the case of multiple-disk is just the iterative utilization of Eq. (37) with an additional tilt factor, when we proved that the gradient diffraction wave was to be neglected. The analytical propagator presents lots of improvement on simplification and efficiency than former numerical propagators, and hence, is of great significance to future external coronagraph design and analysis, especially the initial design process with less time-consuming. Nevertheless, the work in this paper only gives the solution for on-axis diffraction case. For application in solar coronagraphs, further extension of the propagator to off-axis case should be developed. These developments are left for a further study.

Funding

National Natural Science Foundation of China (61705220); Youth Innovation Promotion Association of the Chinese Academy of Sciences (2019219).

Disclosures

The authors declare no conflicts of interest.

Optics EXPRESS

References

1. G. Newkirk Jr and D. Bohlin, "Reduction of scattered light in the coronagraph," Appl. Opt. **2**(2), 131–140 (1963).
2. R. M. MacQueen, A. Csoeke-Poeckh, E. Hildner, L. House, R. Reynolds, A. Stanger, H. Tepoel, and W. Wagner, "The High Altitude Observatory Coronagraphy Polarimeter on the Solar Maximum Mission," Sol. Phys. **65**(1), 91–107 (1980).
3. G. E. Brueckner, R. A. Howard, M. J. Koomen, C. M. Korendyke, D. J. Michels, D. G. Socker, K. P. Dere, P. L. Lamy, A. Llebaria, M.-V. Bout, R. Schwenn, G. M. Simnett, D. K. Bedford, and D. J. Eyles, "The Large Angle Spectroscopic Coronagraph ~LASCO," Sol. Phys. **162**(1-2), 357–402 (1995).
4. R. A. Howard, J. D. Moses, A. Vourlidas, J. S. Newmark, D. G. Socker, S. P. Plunkett, C. M. Korendyke, J. W. Cook, A. Hurley, J. M. Davila, W. T. Thompson, O. C. St Cyr, E. Mentzell, K. Mehalick, J. R. Lemen, J. P. Wuelser, D. W. Duncan, T. D. Tarbell, C. J. Wolfson, A. Moore, R. A. Harrison, N. R. Waltham, J. Lang, C. J. Davis, C. J. Eyles, H. Mapson-Menard, G. M. Simnett, J. P. Halain, J. M. Defise, E. Mazy, P. Rochus, R. Mercier, M. F. Ravet, F. Delmotte, F. Auchere, J. P. Delaboudiniere, V. Bothmer, W. Deutsch, D. Wang, N. Rich, S. Cooper, V. Stephens, G. Maahs, R. Baugh, D. McMullin, and T. Carter, "Sun Earth Connection Coronal and Heliospheric Investigation (SECCHI)," Space Sci. Rev. **136**(1-4), 67–115 (2008).
5. R. Rougeot, R. Flamary, D. Galano, and C. Aime, "Performance of the hybrid externally occulted Lyot solar coronagraph - Application to ASPIICS," Astron. Astrophys. **599**, A2 (2017).
6. C. Aime, "Theoretical performance of solar coronagraphs using sharp-edged or apodized circular external occulters," Astron. Astrophys. **558**, A138 (2013).
7. C. Aime, "Fresnel diffraction of multiple disks on axis - Application to coronagraphy," Astron. Astrophys. **637**, A16 (2020).
8. A. V. Lenskii, "Theoretical evaluation of the efficiency of external occulting systems for coronagraphs," Astron. Zh. **58**, 648–659 (1981).
9. R. Rougeot and C. Aime, "Theoretical performance of serrated external occulters for solar coronagraphy -Application to ASPIICS," Astron. Astrophys. **612**, A80 (2018).
10. E. Cady, "Boundary diffraction wave integrals for diffraction modeling of external occulters," Opt. Express **20**(14), 15196–15208 (2012).
11. W. Wang, X. Zhang, Q. Meng, and Y. Zheng, "Propagation analysis of phase-induced amplitude apodization optics based on boundary wave diffraction theory," Opt. Express **25**(21), 25992–26001 (2017).
12. W. R. Kelly, E. L. Shirley, A. L. Migdall, S. V. Polyakov, and K. Hendrix, "First- and second-order Poisson spots," Am. J. Phys. **77**(8), 713–720 (2009).
13. E. L. Shirley, "Higher-order boundary-diffraction-wave formulation," J. Mod. Opt. **54**(4), 515–527 (2007).
14. K. Miyamoto, "Effect of boundary diffraction wave in coronagraph," J. Opt. Soc. Am. **54**(9), 1105–1108 (1964).
15. Y. Z. Umul, "Uniform boundary diffraction wave theory of Rubinowicz," J. Opt. Soc. Am. A **27**(7), 1613–1619 (2010).
16. M. Born and E. Wolf, *Principles of Optics* (Cambridge University, 1999).
17. T. Suzuki, "Extension of the Theory of the Boundary Diffraction Wave to Systems with Arbitrary Aperture-Transmittance Function," J. Opt. Soc. Am. **61**(4), 439–445 (1971).